

Error Identification and Recovery in Robotic Snap Assembly

Yusuke Hayami¹, Weiwei Wan¹, Keisuke Koyama¹, Peihao Shi¹, Juan Rojas² and Kensuke Harada¹

Abstract— Existing methods for predicting robotic snap joint assembly cannot predict failures before their occurrence. To address this limitation, this paper proposes a method for predicting error states before the occurrence of error, thereby enabling timely recovery. Robotic snap joint assembly requires precise positioning; therefore, even a slight offset between parts can lead to assembly failure. To correctly predict error states, we apply functional principal component analysis (fPCA) to 6D force/torque profiles that are terminated before the occurrence of an error. The error state is identified by applying a feature vector to a decision tree, wherein the support vector machine (SVM) is employed at each node. If the estimation accuracy is low, we perform additional probing to more correctly identify the error state. Finally, after identifying the error state, a robot performs the error recovery motion based on the identified error state. Through the experimental results of assembling plastic parts with four snap joints, we show that the error states can be correctly estimated and a robot can recover from the identified error state.

I. INTRODUCTION

Robotic product assembly has recently been introduced to some production processes. However, we often encounter products that are difficult for robots to assemble with a high success rate. In this context, this research focuses on the robotic assembly of plastic parts that include snap joints, hereafter called robotic snap assembly, which is often difficult owing to the elasticity of parts. Plastic parts with snap joints are easy to assemble but highly difficult to disassemble; consequently, it becomes crucial to correctly predict assembly failure before the assembly actually fails. Moreover, the deviation in the position of the part, which causes the assembly failure, is usually minute; thus, it becomes difficult for a vision sensor to predict assembly failure. To address this problem, this research proposes a method for error identification and recovery in robotic snap assembly based on 6D force/torque sensor information attached at the wrist. An overview of our proposed method is shown in Fig. 1.

Thus far, a few researchers have proposed methods for identifying error states in robotic snap assembly using force/torque information [1], [2], [3], [4], [5], [6], [7], [8], [9], [10], [11], [12], [13], [14]. However, in all of those methods, the error was identified after completing the assembly task; consequently it becomes difficult to recover from the error state. In contrast, this paper proposes a method for identifying an error state among multiple possible error states during robotic snap assembly. To identify an error state, we

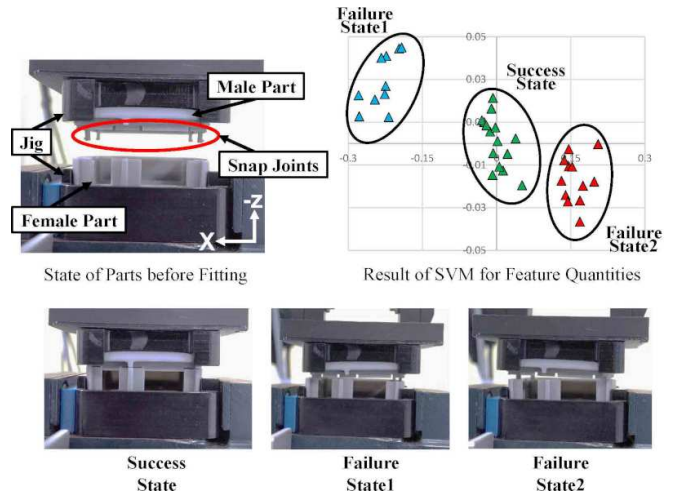


Fig. 1: Identification of success/error states in robotic snap assembly

apply functional principal component analysis (fPCA) to the force/torque profile of an assembly task. Furthermore, to identify an error state among multiple possible error states, we construct a decision tree wherein the classification of the force/torque profile is performed at each node with the support vector machine (SVM) by employing the kernel function. In addition, if the estimation accuracy is not sufficiently high, we perform additional probing, whereby the part is moved to more correctly identify the error state. After the error state is identified, a robot retries the assembly task by slightly modifying the initial position/orientation of the part in the direction opposite to that in the identified error state.

The remainder of this paper is organized as follows: A few relevant previous works are described in Section 2, the proposed method is elucidated in Section 3, and we present our experimental results in Section 4. Finally, summary and scope for further research are presented in Section 5.

II. RELATED WORK

Robotic assembly has been researched for decades [15], [16], [17], [18]. The research on robotic assembly has been mainly done on force controlled assembly [15], [16], assembly motion planning [17], [18], [19], [20], [21], learning based methods [22], [23], and gripper design [24].

Recently, the discrimination of failure states in robotic assembly tasks has been studied by some researchers such as [1][2][3][4][5][6][7]. Rodrigues et al. [1] identified assembly failure using the SVM and PCA. Rojas et al.

¹Graduate School of Engineering Science, Osaka University; 1-3 Machikaneyama-cho, Toyonaka, Osaka 560-8531, JAPAN harada@sys.es.osaka-u.ac.jp

² Chinese University of Hong Kong

[8][9][10][11][12][13] identified an error state among multiple possible states using relative-change-based hierarchical taxonomy (RCBHT). Lello et al. [14] discriminated success/failure of snap assembly based on Bayesian structural time series. However, in all the previous studies, the force/torque profile that is obtained upon the completion of the assembly is used, and it is impossible to predict an error state among multiple possible states before the error actually occurs.

With respect to the robotic manipulation researches on recovery from error states, some researchers [25], [26] used tactile information to identify and recover from the error states. On the other hand, this research uses a 6D force/torque sensor attached at the wrist during a snap joint assembly to recover from the identified error state.

III. PROPOSED METHOD

The proposed method is composed of offline and online phases. In the offline phase, we collect the training data, that is, the force/torque profiles obtained by using the 6D force/torque sensor attached at the wrist during robotic snap assembly, and construct the decision tree for classifying error states. In the online phase, based on a given force/torque profile corresponding to a snap assembly that was terminated before the error actually occurred, we predict an error state using the constructed decision tree. If the accuracy of prediction is not sufficiently high, we perform additional probing by moving the part to more correctly identify the error state. After the error state is identified, a robot tries to recover from it. The robot retries the assembly task by modifying the initial position/orientation of the part in the direction opposite to that in the identified error state.

A. Problem Definition

We consider the assembly of plastic parts with four snap joints, as shown in Fig. 1. In robotic snap assembly, a robot holds the male part, including the snap joints, and moves in the $+z$ (horizontally downward) direction to fit this part to the corresponding female part. During assembly, we obtain the 6D force/torque information using a force/torque sensor attached at the robot wrist. We perform assembly experiment by shifting the initial position/orientation of the male part by various values. We call such deviation of initial position/orientation in multiple directions as the offset pattern. For simplicity, this research considers the offset patterns assuming the x -directional translation (Δx) and the rotation about the x -axis ($\Delta\theta_x$). Based on the 6D force/torque profile of a snap assembly, we determine (1) assembly success or the directional offset, that causes assembly failure, which is categorized as

- | | |
|--|--|
| (2) $\Delta x \geq 0$, | (3) $\Delta x \leq 0$ |
| (4) $\Delta\theta_x \geq 0$, | (5) $\Delta\theta_x \leq 0$ |
| (6) $\Delta x \geq 0, \Delta\theta_x \geq 0$, | (7) $\Delta x \geq 0, \Delta\theta_x \leq 0$ |
| (8) $\Delta x \leq 0, \Delta\theta_x \geq 0$, and | (9) $\Delta x \leq 0, \Delta\theta_x \leq 0$. |

We especially consider directional offsets (2) \dots (9) as the error states. Thus, this research predicts the assembly success and error states (1) \dots (9) using the assembly force/torque profile.

B. Construction of decision tree

To classify error states based on the force/torque information, we define the feature vector composed of the principal component score obtained via functional principal component analysis (fPCA). Using the obtained feature vector, we construct the decision tree to classify error states.

1) *Data collection*: We collect the force/torque profile during the assembly task to construct the decision tree for the purpose of identifying error states. We assume that there are N offset patterns with regard to the initial position/orientation of the male part. Then, the male part is moved in the $+z$ direction so that it can be fit to the female part to check whether the assembly succeeded or not.

2) *Feature extraction*: In this subsection, we explain the manner in which the feature quantities are defined using the 6D force/torque profile. Let the time trajectory of each force/torque component corresponding to the i -th offset pattern be $f_i(t)$. We apply fPCA [27] to $f_i(t)$. Among the principal component $\xi(s)$ satisfying the following equation, we collect p from the one with the largest eigenvalue of ρ .

$$\int v(s,t)\xi(s)dt = \rho\xi(t),$$

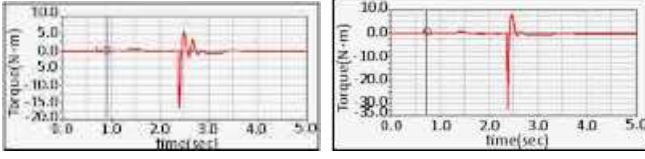
$$v(s,t) = \frac{1}{N} \sum_{i=1}^N (f_i(s) - \bar{f}(s))(f_i(t) - \bar{f}(t)),$$

where $v(s,t)$ denotes the covariance matrix. We can now define a p -dimensional feature vector for each force/torque component corresponding to the i -th offset pattern. Here, if we consider a single $6p$ -dimensional feature vector, the error classification may depend on some specific force/torque components. Hence, we consider six p -dimensional feature vectors where the SVM is separately applied to each force/torque component.

3) *Decision tree based on SVM*: In this subsection, we elucidate the construction of the decision tree for classifying error states. Here, depending on the error state, the component of force/torque that can enable the classification of the error state is different. For example, let us consider the force/torque profiles corresponding to two assembly tasks with different offset patterns shown in Figs. 2 and 3. If we compare the torques about the y -axis, it becomes extremely difficult to differentiate between two offset patterns, as shown in Fig. 2. However, if we compare the torques about the x -axis, we can easily differentiate between two offset patterns, as shown in Fig. 3.

Based on this observation, we construct a decision tree wherein we divide the training data included in the each node into two groups by referring to an appropriate force/torque component. The algorithm employed for constructing the decision tree is described in Algorithm 1.

In the initial state, the decision tree is composed only of the root node that includes all the training data. In this node, we iteratively apply the training data corresponding to each force/torque component to the SVM to split the training data into two groups such that the highest accuracy is obtained.



(a) Torque about y axis:1 (b) Torque about y axis:2

Fig. 2: Torque about y axis obtained through experiments with two different error states



(a) Torque about x axis:1 (b) Torque about x axis:2

Fig. 3: Torque about x axis obtained through experiments with two different error states

If we can find such force/torque component, we add two children nodes and split the training data into two groups. We iterate these steps until we can classify each error state. We calculate the accuracy of classification based on the following equation:

$$Accuracy = \frac{\frac{\sum P_{TP} + \sum P_{FP}}{TP + FN} + \frac{\sum P_{FN} + \sum P_{TN}}{FP + TN}}{2}, \quad (1)$$

where TP, FP, TN and FN denote the true positives, false positives, true negatives and false negatives, respectively, corresponding to the feature quantities, and P_* denotes the class probability of $*$ based on the output of SVM.

C. Identification of error states and error recovery

In this subsection, we present the identification of an error state before the error actually occurs, after which a robot tries to recover from the error state. The identification of error states in this study includes two steps. In the first step, the male part is moved in the $+z$ direction so that it can be fit to the female part; this will hereafter be called the assembly motion. Before the error actually occurs, the robot stops moving the male part and attempts to identify an error state. However, if the class probability is not high enough, we move on to the second step. In the second step, we perform additional probing to identify the error state with a higher probability.

During the assembly motion, we obtain the 6D force/torque profile, which is terminated before the error actually occurs. Using this profile, we obtain the feature vectors as described in subsection III-B.2. The feature vector is applied to the decision tree elucidated in subsection III-B.3. We check the class probability of all the nodes employed to identify the error state. If the class probability of at least one of the nodes is lower than the threshold, it is difficult to correctly estimate the error state. In this case, the male part entails additional probing to identify the error state more correctly. It first moves in the $+x$ direction and then in the

Data: fPCA scores and success/error states
 Success pattern index: $i \leftarrow 0$
 Error pattern index: $i \leftarrow 1, \dots, F$
 Force/torque component: $j \leftarrow 1, \dots, 6$
 Index of waveform data: $k \leftarrow 1, \dots, N(i)$
 Waveform data: $WD(i, j, k)$
 Combinations of success/error states: C

Result: Construction of a decision tree

```

begin
  id ← 0
  node(id).pattern_id ← [0, 1, …, F]
  max_id ← 0
  while 1 do
    if size(node(id).pattern_id == 1) then
      if id == max_id then
        return node
      end
      id ← id + 1
      continue
    end
    for j ← 1, …, 6 do
      for  $\forall C \subset$  node(id).pattern_id do
        i ← node(id).pattern_id,
        patterns(j, C) ←
          SVM(fPCAScore(WD(i, j, k)), C)
        accuracy(j, C) ←
          calcAccuracy(patterns(j, C))
      end
    end
    node(id).component ←
      argmaxj(accuracy(j, C))
    node(id).patterns ← argmaxC(accuracy(j, C))
    node(id).children ← [max_id + 1, max_id + 2]
    node(max_id + 1).pattern_id ←
      node(id).patterns
    node(max_id + 2).pattern_id ←
      node(id).pattern_id - node(id).patterns
    max_id ← max_id + 2
  end
end

```

Algorithm 1: Classifier constructed based on SVM

$-x$ direction. We note that we have also constructed decision trees for additional probing in $+x$ and $-x$ directions in the offline phase. We obtain the 6D force/torque profiles for both cases, and then apply the feature vector to the decision tree to more accurately identify the error state. We apply the identification result with the higher accuracy, calculated using eq.(1) of the node with the smallest accuracy.

Finally, in this section, the method for error recovery is explained as follows: If the assembly is predicted to be successful, the male part is further moved in the $+z$ direction and fit to the female part. If an error state is identified, the male part is moved once in the $-z$ direction and then moved by a fixed (small) distance in the direction opposite to that in the identified error state. Then, the male part is moved in

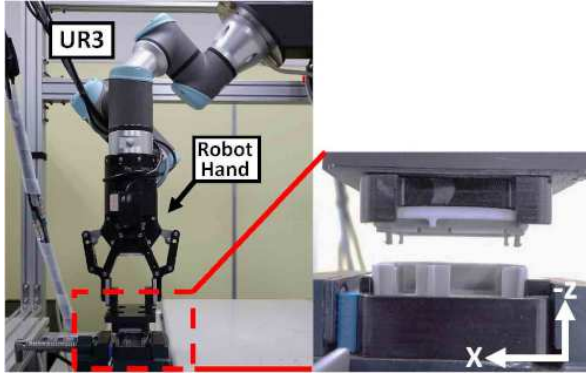


Fig. 4: Experimental environment



(a) Male part

(b) Female part

Fig. 5: Assembly parts

the $+z$ direction again to fit it to the female part.

IV. EXPERIMENT

This section details the experiment conducted to demonstrate the effectiveness of the proposed approach.

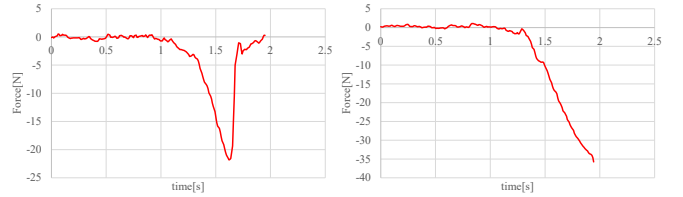
A. Experimental environment

Our experimental setup is shown in Fig. 4. We used UR3 with a Robotiq 6D force/torque sensor attached at the wrist. To avoid the application of an excessively large force at the wrist, we also installed a compliant mechanism at the wrist (SHM61J, Koganei Co., Ltd.). The plastic parts with four snap joints used for assembly are shown in Fig. 5.

B. Force/torque data

We performed assembly experiment with 131 offset patterns assuming different initial position/orientation of the male part in the range of $-2.0[\text{mm}] \leq \Delta x \leq 2.0[\text{mm}]$, $-2.0[\text{deg}] \leq \Delta \theta_z \leq 2.0[\text{deg}]$. In an assembly task, the male part is first moved $6[\text{mm}]$ to the $+z$ direction, and the error states are identified. If additional probing is required, the male part is first moved $1[\text{mm}]$ to the $-z$ direction and then $2[\text{mm}]$ to the $\pm x$ directions. The threshold of the class probability introduced in subsection III-C is set at 0.2. To recover from an error state, the male part is moved $1[\text{mm}]$ and $1[\text{deg}]$ in the opposite direction of the identified error state.

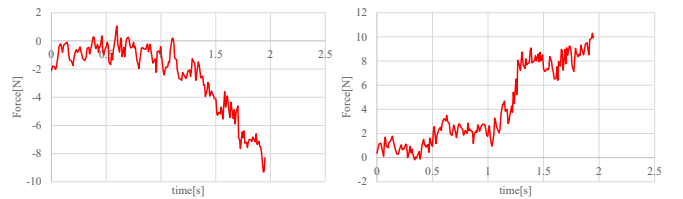
Under the condition given in subsection IV-A, we collected both training and validation data. The obtained force/torque profiles of the characteristic components are shown in Figs. 6, 7 and 8. We can observe that the force/torque profile differ



(a) Successful case (1)

(b) Error state (6)

Fig. 6: Force in z direction obtained through experiment of successful and failure cases



(a) Error state (7)

(b) Error state (8)

Fig. 7: Force in x direction obtained through experiment of different error states

between the error states. Specifically, the force profile in the z direction can be used to discriminate successful cases from failure cases. A successful case of assembly is shown in Fig. 9, where (a) and (b) show the male part's motion in the $+z$ direction and (c) and (d) show the additional probing in the $\pm x$ directions. The failure case of assembly is shown in Fig. 10.

C. Feature extraction

From a given force/torque profile of a snap assembly, we extracted the force/torque profile terminated at time t_{span} . Then, for the extracted force/torque profile terminated at t_{span} , we calculated the feature vector. Fig. 11 shows the plot of the 1st and 2nd functional principal component scores assuming $t_{span} = 2.0[\text{s}]$ (before the error actually occurs). By observing this plot, some error states seem to be classified depending on the force/torque component, e.g., the blue circle of the force in the z -direction. To form the decision tree, we will try to find such force/torque component that can accurately classify the error state. In our experiment, with the 1st and 2nd functional principal components, the contribution rate exceeded 90%.

D. Construction of the decision tree

We constructed a decision tree using the feature vector obtained in subsection IV-C with the leave-one-out cross validation. In each node of the tree, we classified the error state by using the SVM with the kernel function. For the case of $t_{span} = 2.0[\text{s}]$, the decision tree constructed and the feature vectors classified using the SVM are shown in Figs. 12 and 13, respectively.

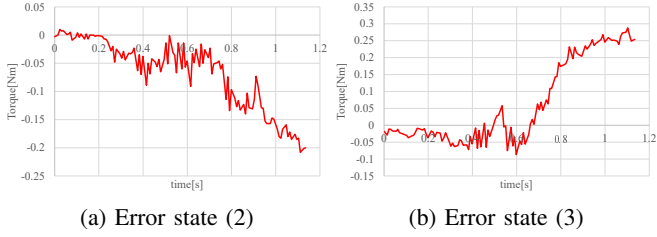


Fig. 8: Torque about x axis obtained through experiment of different error states with additional probing in the $+x$ direction

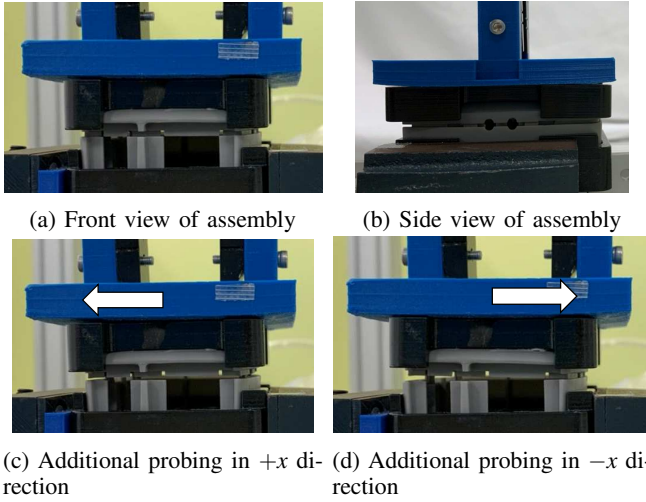


Fig. 9: Snapshots of successful snap assembly ($\Delta y = 0[\text{mm}]$, $\Delta\theta_z = 0.5[\text{deg}]$)

TABLE I: Classification accuracy (eq.(1)) of error states calculated at each node of decision tree [%]

Node number	$t_{span} = 1.8[\text{s}]$	1.9 [s]	2.0 [s]
Node1	95.8	95.5	98.0
Node2	94.1	96.1	95.9
Node3	95.2	94.8	95.5
Node4	85.5	91.2	85.7
Node5	91.1	90.8	91.9
Node6	86.4	86.7	84.2
Node7	90.5	91.9	89.9
Node8	90.5	85.9	83.4

The classification accuracies in the cases $t_{span} = 1.8, 1.9$ and $2.0[\text{s}]$ are shown in Table I. The table indicates that the classification accuracy exceeds 85% in most cases. Specifically, the accuracy is relatively high in all the nodes of $t_{span} = 1.9[\text{s}]$. These results imply that, by selecting an appropriate t_{span} , error states can be estimated with the classification accuracy between 85 and 95 % even before errors actually occur.

E. Identification of error states

By using the validation data obtained in subsection IV-B, we checked how early we can identify error states assuming $t_{span} = 1.8, 1.9$ and $2.0[\text{s}]$. The validation data include 45 successful and 40 error cases. The result of error-state

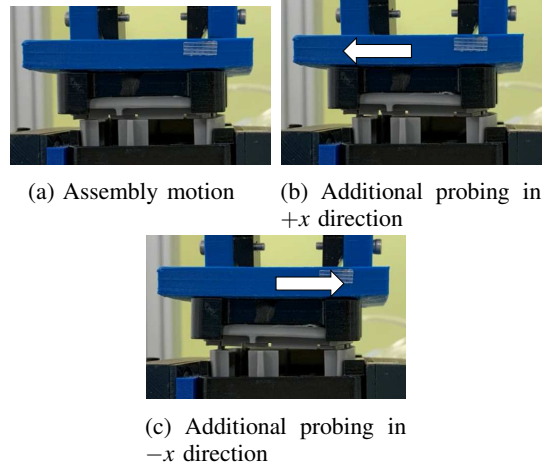


Fig. 10: Snapshots of snap assembly failure ($\Delta y = 1.5[\text{mm}]$, $\Delta\theta_z = 1.5[\text{deg}]$)

TABLE II: Classification result of success/error states in the assembly motion where the male part moves in the $+z$ direction

$t_{span} [\text{s}]$	Number of successful identification	Success rate(%)
1.8	74	87.1
1.9	84	98.8
2.0	83	97.6

identification for assembly motion when the male part moves in the $+z$ direction is presented in Table II. The success rate of classification exceeds 87%.

Then, the result of classification when performing additional probing in the $\pm x$ direction is presented in Table III. The success rate of classification by additional probing itself is not very high. Furthermore, Table IV shows the success rate of classification achieved by additional probing in the $\pm x$ direction performed only when the classification accuracy of assembly motion is less than the threshold. In this case, the success rate of classification exceeds 92%, which demonstrates the effectiveness of using additional probing. The result of classification of each error state corresponding to $t_{span} = 2.0[\text{s}]$ is presented in Table V.

Table II indicates that the accuracies of error-state identification were 87.1%, 98.8%, and 97.6% when $t_{span} = 1.8, 1.9$ and $2.0 [\text{s}]$, respectively. From this observation, without information included between $t_{span} = 1.8$ and $1.9[\text{s}]$ it becomes difficult to identify error states. t_{span} should be set larger than $1.9 [\text{s}]$.

F. Error recovery

We implemented the recovery motion from the identified error state. In this experiment, we tested the error recovery three times each for the following three cases:

- After identified as the successful case (1), a robot further moves the male part in the $+z$ direction, and

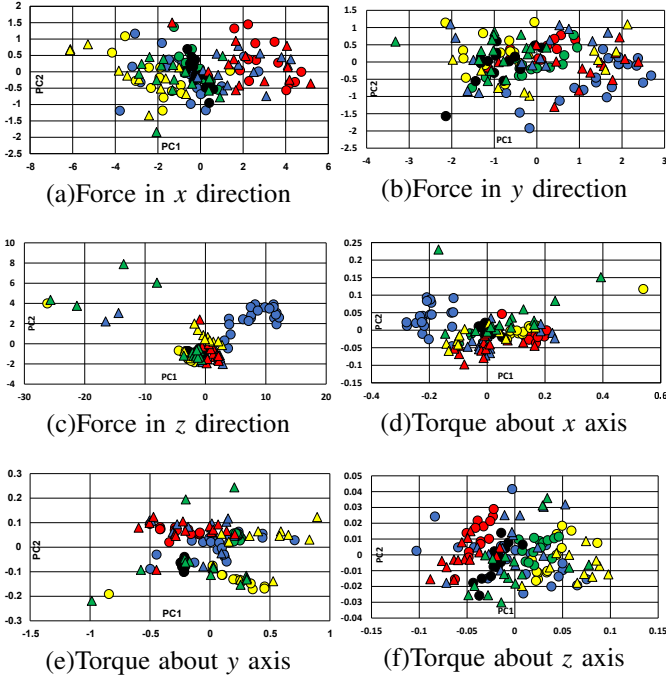


Fig. 11: Plots of functional principal component scores during snap assembly terminated at $t_{span} = 2.0[s]$, where blue, red, yellow, green and black circles, and blue, red, yellow and green triangles denote the success/error states (1), \dots , (9), respectively.

TABLE III: Classification result of success/error states with using the additional probing

Number of successful identification	Success rate(%)
63	74.1

the task ($\Delta x = 0.5[mm]$, $\Delta\theta_z = 0.5[deg]$) is completed. Apparently, a robot does not need to recover from the error state in this case.

- (b) After an error state is identified, a robot attempts to recover from the error state($\Delta x = 1.5[mm]$, $\Delta\theta_z = -1.5[deg]$).
- (c) After an error state is identified, a robot performs the additional probing. Then, a robot attempts to recover from the error state($\Delta x = -1.5[mm]$, $\Delta\theta_z = -1.5[deg]$).

Among three cases, a robot recovers from the identified error states in the cases (b) and (c). The snapshots of error recovery motion are shown in Figs. 14, 15 and 16 corresponding to the cases (a), (b) and (c), respectively. We tried the error recovery for three times for each case. The robot could successfully recover from the error state in all the cases without breaking the part, as shown in Table VI.

V. CONCLUSION

In this paper, we proposed a method of predicting error states before the error actually occurs in robotic snap assembly for recovering from the identified error state. We perform the functional principal component analysis (fPCA) of the

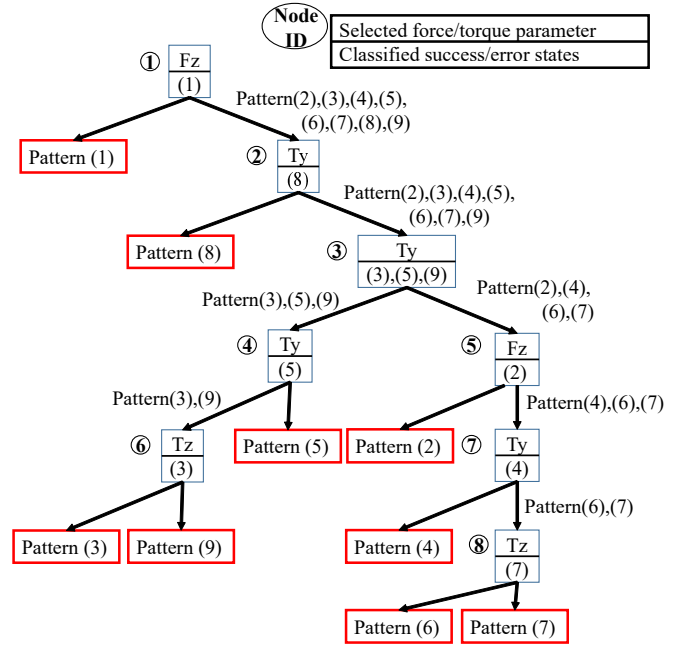


Fig. 12: Decision tree of the snap assembly terminated at $t_{span} = 2.0[s]$

TABLE IV: Classification result of success/error states with using the additional probing after the assembly motion where the male part moves in the $+z$ direction

$t_{span}[s]$	Improved identification	Deteriorated identification	Identification Succeeded	Success rate(%)
1.8	9	4	79	92.9
1.9	0	0	84	98.8
2.0	2	0	85	100

6D force/torque profile. We confirmed that an error state is correctly identified by applying the obtained feature vector to the decision tree. We also confirmed that, if the estimation accuracy is low, we could better identify the error state by additional probing. After identifying the error state, a robot successfully attempted to recover from the identified error state.

In this paper, we confirmed the effectiveness of our approach by using a plastic parts with four snap joints. Application of our proposed method to other parts with different shape is considered to be our future research topic. In addition, we assumed just Δx and $\Delta\theta_z$ to define the error states. As we increase the number of error states, it will become difficult to correctly estimate the error states. In a future research, we would increase the number of error states and see the estimation accuracy. The accuracy of estimation might depends also on the dynamics of the parts. Consideration on the dynamic effect is considered to be our future research topic.

REFERENCES

- [1] A. Rodriguez, D. Bourne, M. Mason, G. F. Rossano, and J. Wang, "Failure detection in assembly: Force signature analysis," in 2010

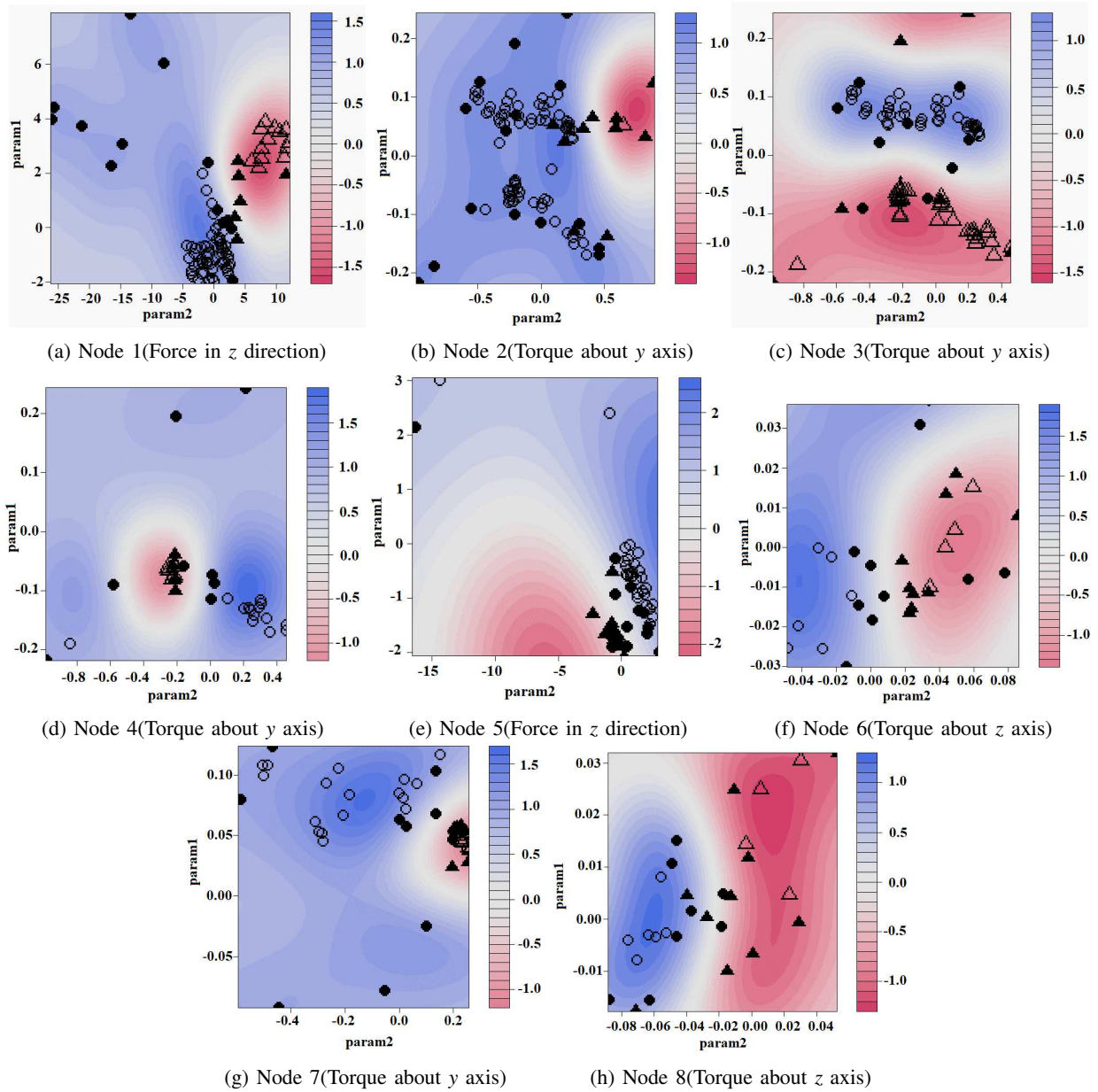


Fig. 13: Classification result of error states by using SVM corresponding to feature quantities shown in Fig.12

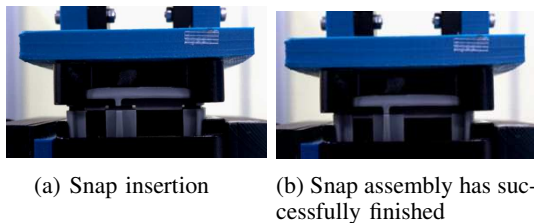


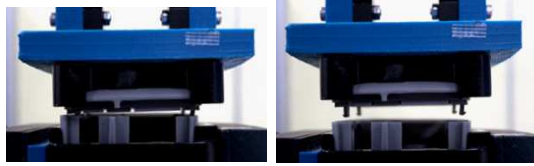
Fig. 14: Error recovery from the offset pattern (1)

- IEEE Int. Conf. on Automation Science and Engineering*, 2010, pp. 210–215.
- [2] A. Stolt, M. Linderöth, A. Robertsson, and R. Johansson, “Detection of contact force transients in robotic assembly,” in *2015 IEEE Int. Conf. on Robotics and Automation*, 2015, pp. 962–968.
- [3] M. Ge, Y. Xu, and R. Du, “An intelligent online monitoring and

- diagnostic system for manufacturing automation,” *IEEE Trans. on Automation Science and Engineering*, vol. 5, no. 1, pp. 127–139, 2008.
- [4] L. Rusli, A. Luscher, and C. Sommerich, “Force and tactile feedback in preloaded cantilever snap-fits under manual assembly,” *Int. J. of Industrial Ergonomics*, vol. 40, no. 6, pp. 618 – 628, 2010.
- [5] G. Suat, R. W. Messler, and G. A. Gabriele, “A hierarchical classification scheme to define and order the design space for integral snap-fit assembly,” *Research in Engineering Design*, vol. 10, pp. 94–106, 1998.
- [6] J. Ji, K.-M. Lee, and S. Zhang, “Cantilever snap-fit performance analysis for haptic evaluation,” *J. of Mechanical Design*, vol. 133, p. 121004, 12 2011.
- [7] S. Cho, S. Asfour, A. Onar, and N. Kaundinya, “Tool breakage detection using support vector machine learning in a milling process,” *International Journal of Machine Tools and Manufacture*, vol. 45, no. 3, pp. 241 – 249, 2005.
- [8] J. Rojas, K. Harada, H. Onda, N. Yamanobe, E. Yoshida, K. Nagata, and Y. Kawai, “A relative-change-based hierarchical taxonomy for cantilever-snap assembly verification,” in *2012 IEEE/RSJ Int. Conf. on Intelligent Robots and Systems*, 2012, pp. 356–363.

TABLE V: Result of identification for successful/error states calculated at $t_{span} = 2.0[s]$

Success /error states	Δx [mm]	$\Delta \theta_z$ [deg]	Success rate (assembly) [%]	Success rate (probing) [%]	Success rate (probing after assembly) [%]
(1)	-0.25	-0.25	80	80	100
(1)	-0.5	0.5	100	100	100
(1)	-0.5	0	100	100	100
(1)	0.25	-0.25	100	20	100
(1)	0.5	0.5	100	100	100
(1)	0.5	0	100	0	100
(1)	0	-0.5	100	40	100
(1)	0	0.5	100	80	100
(1)	0	0	100	20	100
(2)	2	0	100	100	100
(3)	-2	0	80	100	100
(4)	0	2	100	100	100
(5)	0	-2	100	100	100
(6)	1.5	1.5	100	100	100
(7)	1.5	-1.5	100	60	100
(8)	-1.5	1.5	100	60	100
(9)	-1.5	-1.5	100	100	100



(c) Snap assembly has successfully finished

Fig. 15: Error recovery from the offset pattern (2)

- [9] J. Rojas, K. Harada, H. Onda, N. Yamanobe, E. Yoshida, and K. Nagata, "Early failure characterization of cantilever snap assemblies using the pa-rcbht," in *2014 IEEE Int. Conf. on Robotics and Automation (ICRA)*, 2014, pp. 3370–3377.
- [10] J. Rojas, K. Harada, H. Onda, N. Yamanobe, E. Yoshida, K. Nagata, and Y. Kawai, "Cantilever snap assembly automation using a constraint-based pivot approach," in *IEEE Int. Conf. on Mechatronics and Automation*, 2012.
- [11] J. Rojas, K. Harada, H. Onda, N. Yamanobe, E. Yoshida, K. Nagata, and Y. Kawai, "Probabilistic state verification for snap assemblies using the relative-change-based hierarchical taxonomy," in *2012 IEEE-RAS Int. Conf. on Humanoid Robots*, 2012, pp. 96–103.
- [12] —, "Gradient calibration for the rcbht cantilever snap verification system," in *IEEE Int. Conf. on Robotics and Biomimetics*, 2012, pp. 984–990.
- [13] W. Luo, J. Rojas, T. Guan, K. Harada, and K. Nagata, "Cantilever snap assemblies failure detection using svms and the rcbht," in *IEEE Int. Conf. on Mechatronics and Automation*, 2014, pp. 384–389.
- [14] E. Di Lello, M. Klotzbücher, T. De Laet, and H. Bruyninckx, "Bayesian time-series models for continuous fault detection and recognition in industrial robotic tasks," in *2013 IEEE/RSJ Int. Conf. on Intelligent Robots and Systems*, v 2013, pp. 5827–5833.
- [15] D. E. Whitney, "Force feedback control of manipulator fine motions," *ASME J. of Dyn. Syst., Meas., and Control*, vol. 99, no. 2, p. 91–97, 1977.
- [16] N. Hogan, "Impedance control: An approach to manipulation, part i—iii," *ASME J. on Dyn. Syst., Meas., and Control*, vol. 107, no. 1,

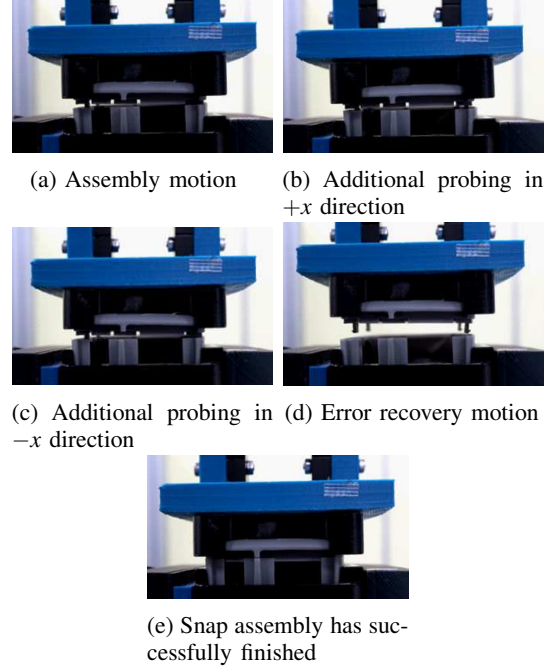


Fig. 16: Error recovery from the offset pattern (3)

TABLE VI: Result of error recovery

Offset pattern	Number of successful case	Success rate
(1)	3	100
(2)	3	100
(3)	3	100

- 1985.
- [17] L. S. H. de Mello and A. C. Sanderson, "Automatic generation of mechanical assembly sequences," *Carnegie Mellon University, the Robotics Institute*, 1988.
- [18] R. H. Wilson and J.-C. Latombe, "Geometric reasoning about mechanical assembly," *Artificial Intelligence*, vol. 71, no. 2, p. 371–396, 1994.
- [19] U. Thomas, T. Stouraitis, and M. A. Roa, "Flexible assembly through integrated assembly sequence planning and grasp planning," in *Proc. of IEEE Int. Conf. on Automation Science and Engineering*, 2015, p. 586–592.
- [20] W. Wan and K. Harada, "Integrated assembly and motion planning using regrasp graph," *Robotics and Biomimetics*, vol. 3, no. 18, 2016.
- [21] M. Dogar, A. Spielberg, S. Baker, and D. Rus, "Multi-robot grasp planning for sequential assembly operations," in *Proc. of IEEE Int. Conf. on Robotics and Automation*, 2015.
- [22] G. Thomas, M. Chien, A. Tamar, J. A. Ojea, and P. Abbeel, "Learning robotic assembly from cad," *arXiv*, 2019.
- [23] C. C. Beltran-Hernandez, D. Petit, I. G. Ramirez-Alpizar, T. Nishi, S. Kikuchi, T. Matsubara, and K. Harada, "Learning contact-rich manipulation tasks with rigid position-controlled robots: Learning to force control," *IEEE Robotics and Automation Letters*, 2020.
- [24] D. Pham and S. Yeo, "Strategies for gripper design and selection in robotic assembly," *Int. J. production research*, vol. 29, no. 2, p. 303–316, 1991.
- [25] H. Dang and P. Allen, "Grasp adjustment on novel objects using tactile experience from similar local geometry," in *Proc. of IEEE/RSJ Int. Conf. on Intelligent Robots and Systems*, 2013.
- [26] M. Li *et al.*, "Learning of grasp adaptation through experience and tactile sensing," in *Proc. of IEEE/RSJ Int. Conf. on Intelligent Robots and Systems*, 2014.
- [27] J. S. Marron, J. O. Ramsay, L. M. Sangalli, and A. Srivastava, "Functional data analysis of amplitude and phase variation," *Statistical Science*, vol. 30, no. 4, pp. 468–484, 2015.